4 CoLoRFulNNLO at work: A determination of α_S

Authors: Adam Kardos, Stefan Kluth, Gábor Somogyi, Zoltán Trócsányi, Zoltán Tulipánt and Andrii Verbytskyi
Corresponding Author: Adam Kardos [kardos.adam@science.unideb.hu]

4.1 Introduction

The most precise determination of fundamental parameters of the Standard Model is very important. One such fundamental parameter is the strong coupling of QCD. Its importance can be gauged by taking a look at the various experiments and configurations where it was measured, for an up to date summary see Ref. [1]. The precise measurement of such a parameter is two-fold difficult. First, high quality data with small and well-controlled uncertainties are needed. Second, high precision calculations are needed from the theory side such that theoretical uncertainties are small as well.

In a theoretical prediction based on calculation in perturbation theory the uncertainty has two main sources: the omission of higher-order terms which are estimated by the renormalization scale and the numerical stability of the integrations. While the dependence on unphysical scales can be, in principle, decreased by including more and more higher-order contributions in the prediction the numerical uncertainty can be intrinsic to the method used to obtain the theoretical prediction. Beside this, the way of comparison of experiment with theory is also affected by another uncertainty. While an experiment measures color-singlet objects, hadrons, the predictions are made in QCD for colorful ones, partons. The assumption of local parton-hadron duality ensures a correspondence between these two up to non-perturbative effects. Non-perturbative effects are power corrections in nature going with some negative power of the collision energy. This means that for an accurate comparison 1) either these effects should be estimated and taken into account 2) or the experiment should have a high enough energy that these contributions become negligible compared to other effects 3) or an observable has to be chosen which is not sensitive to these effects.

To take into account these non-perturbative effects we have to choose from phenomenological [2,3] or analytical models [4]. It is worth to note that none of these models are derived from first principles hence there is still room for improvement. Non-perturbative effects derived from first principles would also be favored because these corrections are to be used in comparisons of predictions to experimental measurements. Currently phenomenological models use several parameters fitted to experimental data thus bias is introduced in the measurement of physical parameters. The calculation of non-perturbative corrections from first principles is also advocated because the only available analytical model seems to be ill-suited for the current precision of theoretical calculations as it was shown in Ref. [5].

In this report we show two approaches how the measurement of a physical parameter, the strong coupling, can be carried out with high precision. Because the used observables allow for such measurements these can be considered as interesting subjects to study in a future electron-positron collider.

4.2 Precision through higher orders

One possible approach to increase the precision of a measurement from the theoretical perspective is to select an observable and refine its prediction by including higher-order contributions

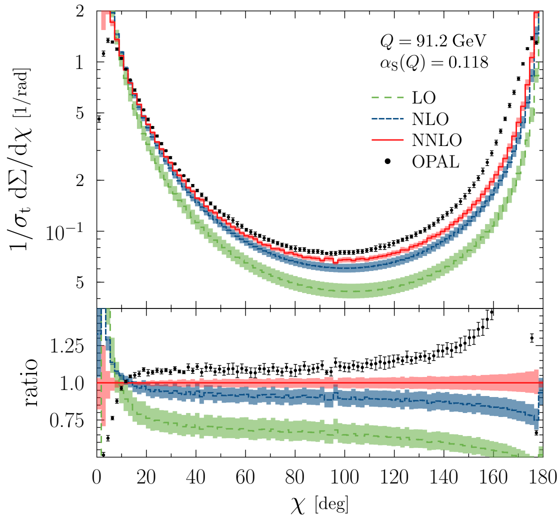

Fig. B.23: The fixed-order prediction for EEC in the first three orders of perturbation theory with theoretical uncertainties. The dots show the measurement by the OPAL collaboration [11]. On the lower panel we compared the predictions and the measurement to the NNLO result.

in fixed-order perturbation theory or by means of resummation. With the completion of the CoLoRFulNNLO subtraction method [6–8] for electron-positron collisions the next-to-next-to-leading order (NNLO) QCD prediction for energy-energy correlation (EEC) became available recently [9] for the first time. Matching this with predictions obtained by resumming leading (LL), next-to-leading (NLL) and next-to-next-to-leading logarithms (NNLL) in the back-to-back region [10] it was possible by matching the two calculations to arrive at the most precise theoretical prediction for this observable at NNLO+NNLL accuracy in QCD [5]. The energy-energy correlation is defined as a normalized energy-weighted sum of two-particle correlations:

$$\frac{1}{\sigma_{\mathrm{t}}}\frac{\mathrm{d}\Sigma(\chi)}{\mathrm{d}\cos\chi} \equiv \frac{1}{\sigma_{\mathrm{t}}}\int\sum_{i,j}\frac{E_i E_j}{Q^2}\mathrm{d}\sigma_{\mathrm{e^+e^-}\to ij+X}\,\delta(\cos\chi+\cos\theta_{ij})\,, \tag{4.37}$$

where Q is the center-of mass energy of the collision, σ_{t} is the corresponding total cross section, E_i is the energy of the ith particle, $\cos\theta_{ij}$ is the enclosed angle between the particles, i and j. The theoretical prediction for EEC in the first three orders of perturbation theory is depicted on Fig. B.23. The theoretical uncertainties were obtained from varying the renormalization scale between $m_Z/2$ and $2m_Z$. As can be seen from the lower panel even when using the highest precision prediction the difference between measurement and theory is sizable. This can be attributed to missing higher-order terms becoming important at the edge of phase space and missing hadronization corrections.

The behavior near $\chi = 0$ can be improved by including all-order results through resummation. In Ref. [12] we used modern Monte Carlo (MC) tools to extract such corrections for EEC. To do so we generated event samples both at the hadron and at the parton level and the ratio of these provided the hadron-to-parton ratio or H/P. Using this ratio and multiplying our parton-level predictions bin-by-bin we obtained our theoretical prediction at the hadron level. As MC tools we used `SHERPA2.2.4` [13] and `Herwig7.1.1` [14]. The exact setup of the MC tools is presented in Ref. [12].

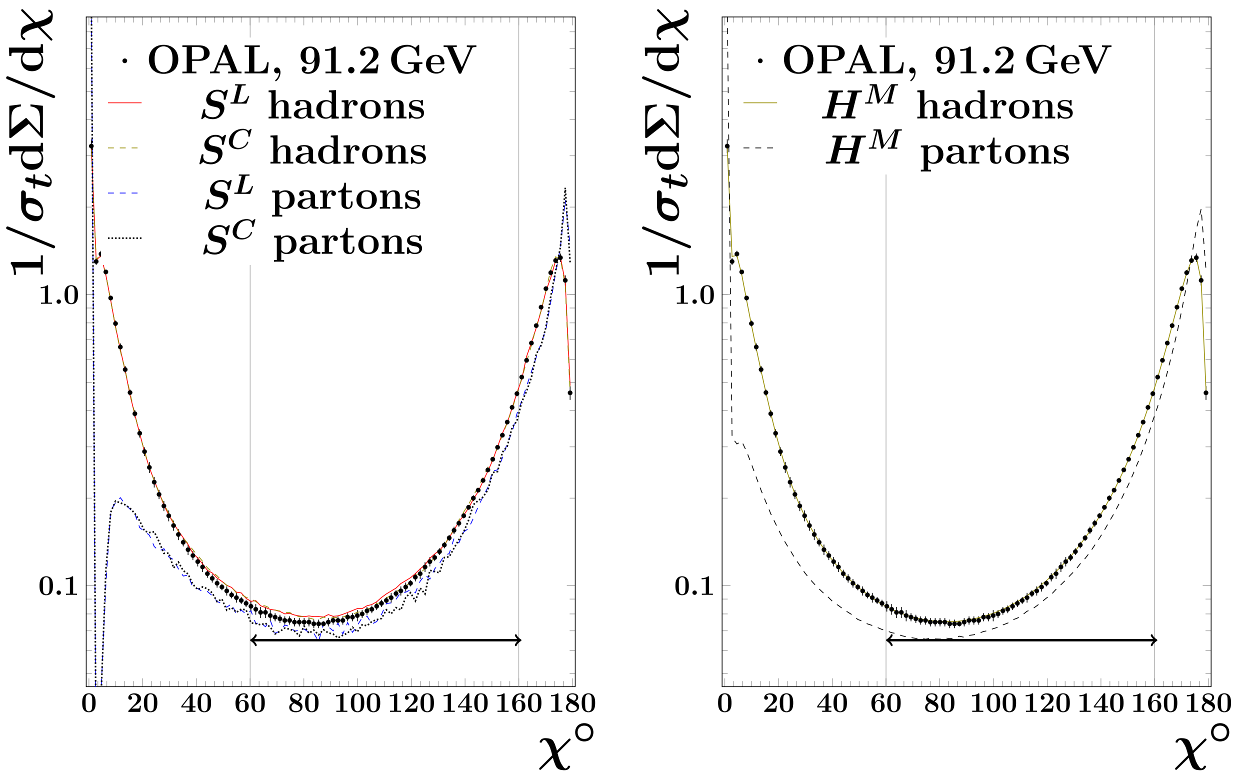

Fig. B.24: EEC distributions obtained with the two MC tools at the parton and hadron level at 91.2 GeV with corresponding OPAL data shown as well. Note that for these two plots a different χ definition was used: this time the back-to-back region corresponds to $\chi \to 180°$.

The value for the strong coupling was determined by fitting the predictions to 20 different data sets, for details see Tab. 1 of Ref. [12]. For illustrative purposes on Fig. B.24 we showed the predictions obtained with `SHERPA` and `Herwig` at the parton and hadron level. For `SHERPA` we used both the Lund (S^L) [3] and cluster (S^C) [2] hadronization models while in `Herwig` we used the built-in cluster model. On the figure we also indicated the range what was used in the actual fitting procedure.

To carry out the fitting the `MINUIT2` program [15] was used to minimize the quantity:

$$\chi^2(\alpha_S) = \sum_{\text{datasets}} \chi^2_{\text{dataset}}(\alpha_S) \tag{4.38}$$

with the $\chi^2(\alpha_S)$[§] quantity calculated as:

$$\chi^2(\alpha_S) = (\boldsymbol{D} - \boldsymbol{P}(\alpha_S))^{\mathrm{T}} \underline{\underline{V}}^{-1} (\boldsymbol{D} - \boldsymbol{P}(\alpha_S)) \,, \tag{4.39}$$

where $\boldsymbol{D}$ is the vector of data points, $\boldsymbol{P}$ is the vector of predictions as functions of α_S and $\underline{\underline{V}}$ is the covariance matrix.

With the fitting procedure performed in the range between 60° and 160°. The resulting strong coupling NNLL+NNLO prediction is:

$$\alpha_S(m_Z) = 0.11750 \pm 0.00287 \tag{4.40}$$

[§]Not to be confused with the angle χ.

and at NNLL+NLO accuracy is:

$$\alpha_{\mathrm{S}}(m_Z) = 0.12200 \pm 0.00535\,. \tag{4.41}$$

Notice the reduction of uncertainties as we go from NNLL+NLO to NNLL+NNLO.

4.3 Precision through small power corrections

As outlined in the introduction the current ways of taking into account the effect of non-perturbative contributions can raise concerns mainly because only phenomenological models are present for them. The other big concern is that these models rely on experimental results through tuned parameters. The best option without any model derived from first principles is to decrease these effects as much as possible. The idea is simple: if the non-perturbative contribution can be shrunk its large uncertainties will become smaller contribution to the final uncertainty of the extracted value of strong coupling.

In this section we focus on altering the definitions of existing observables to decrease the non-perturbative corrections. The most basic and most used observables in electron-positron collisions are the thrust (T) and the various jet masses. In their original definitions all of them incorporate all registered hadronic objects of the event or a given, well-defined region. Hence a natural way to modify these is to filter the tracks contributing to their value in an event. One possible way to remove tracks is by means of grooming [16–21]. In particular the soft drop [21] is a grooming when a part of the soft content of the event is removed according to some criteria.

In Ref. [22] soft-drop variants were defined for thrust, $\tau'_{\mathrm{SD}} = 1 - T'_{\mathrm{SD}}$, hemisphere jet mass, $e_2^{(2)}$ and narrow jet mass, ρ. As it was showed in the paper the non-perturbative corrections can be drastically decreased if soft drop is applied. The effect of soft drop turns out to be the most significant in the peak region of the distributions where the contribution from all-order resummation and non-perturbative effects is the greatest. This makes these observables promising candidates for strong coupling measurements at a future electron-positron collider. The application of these observables – although very interesting – is limited at LEP measurements due to the limited amount of data taken and because the soft-drop procedure inherently results in a decrease of cross section.

In our recent paper [23] we analyzed the proposed observables from the standpoint of perturbative behavior by calculating the NNLO QCD corrections to them and analyzing their dependence on the non-physical renormalization scale as an indicator of the size of neglected higher-order terms. The soft-drop versions of the observables listed above have two parameters related to soft drop: z_c and β [22]. This allows for optimization in order to minimize the decrease in cross section when the soft-drop procedure is applied.

On Fig. B.25 the soft-dropped thrust distribution is shown in the first three orders of QCD perturbation theory for a specific choice of the two soft-drop related parameters. On the right hand side of the same figure the K-factors are depicted for various parameter choices to illustrate the stability of the result. We found that the most stable perturbation prediction and moderate drop in cross section can be achieved when $(z_c, \beta) = (0.1, 0)$.

On Fig. B.26 the soft-dropped hemisphere jet mass is depicted in exactly the same way as the soft-dropped thrust on Fig. B.25. In this case it can be seen once more that the perturbative behavior stabilizes as going to higher orders in perturbation theory. This is the most pronounced at the left hand side of the peak where the NLO and NNLO predictions coincide. For this observable we found that the best choice for the soft-drop parameters is also $(z_c, \beta) = (0.1, 0)$.

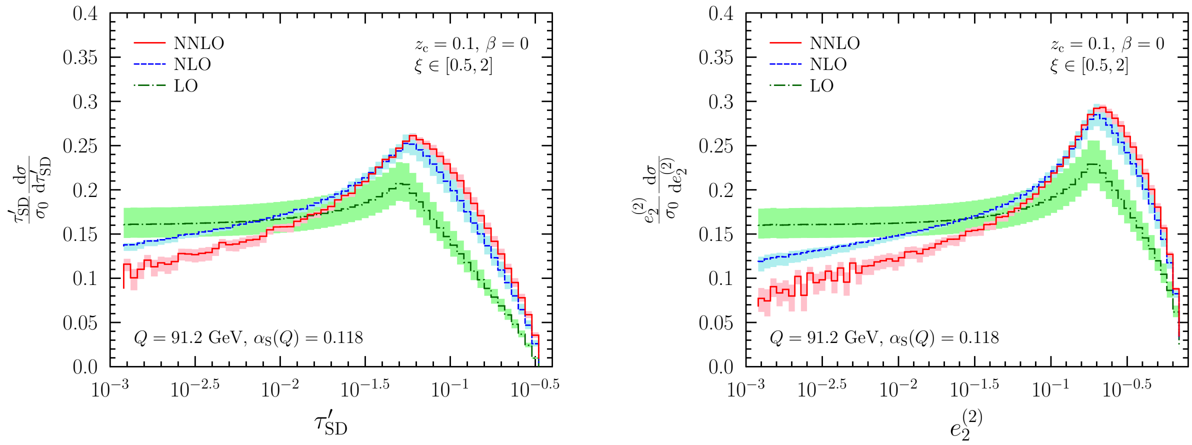

Fig. B.25: (L): Soft-dropped thrust distribution at the Z peak in the first three orders of perturbation theory, the bands represent the uncertainty coming from the variation of the renormalization scale between $Q/2$ and $2Q$. (R): The K-factors for the soft-dropped thrust distribution for various choices of the soft-drop parameters.

For the traditional versions of these observables the peak region is the one where the all-order resummed results and non-perturbative corrections are mandatory to have agreement with the experiment but for the soft-dropped versions neither the higher-order contributions nor the non-perturbative corrections are drastic. The minimal role of higher orders in perturbation theory can be seen from the perturbative stability of our results while the small size of non-perturbative corrections has been shown in Ref. [22]. These properties make the soft-dropped event shapes attractive observables for the extraction of the strong coupling.

4.4 Conclusions

A future electron-positron collider would be considered as a dream machine for many reasons. A machine of this type would allow for a precise tuning of collision energy, it would be without

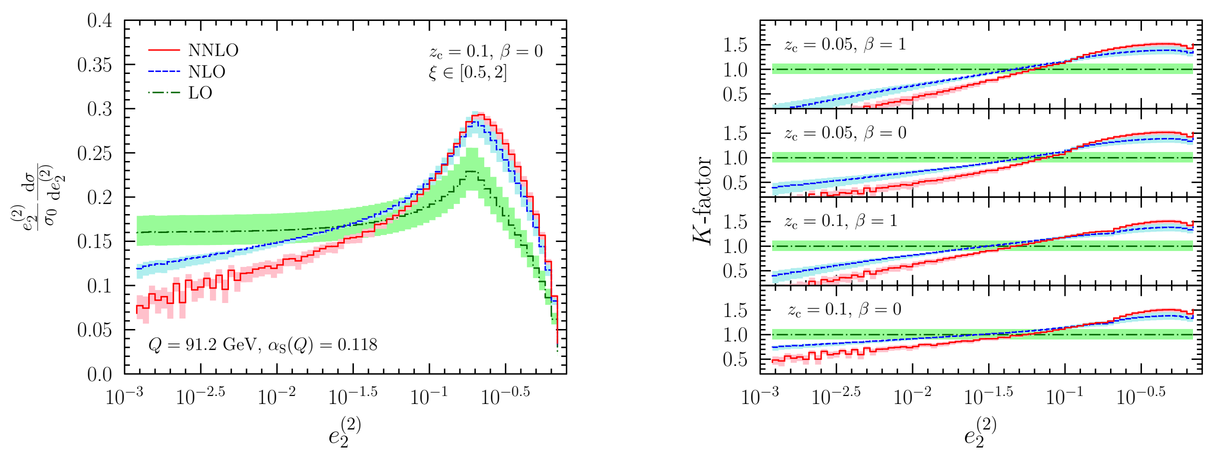

Fig. B.26: The same as Fig. B.25 but for the hemisphere jet mass.

any annoying underlying event and with colored partons in the initial state. Several possible measurements could be envisioned at such a machine but from the QCD point of view the determination of the strong coupling stands out. The strong coupling is a fundamental parameter of the standard model of particle physics so knowing its value is of key importance.

In this report we showed two possible ways to conduct such a measurement. First, by including higher-order corrections in the theoretical prediction and comparing this to the experimental result modeling non-perturbative effects with modern MC tools. Second, we showed modified versions of well-known observables defined in electron-positron collisions where non-perturbative corrections can be minimized hence diminishing the effects of their uncertainties on theoretical predictions. These observables seem to be promising candidates not just for strong coupling measurements but also for the purpose of testing the Standard Model further. Thus they should be seriously considered as important measurements at a future electron-positron facility.

Acknowledgements

A.K. is grateful to the organizers of the FCC-ee 2019 workshop held at CERN for the invitation to give a talk about recent advancements in QCD related to electron-positron colliders and for the warm atmosphere they created.

References

[1] S. Bethke, α_s 2016, Nucl. Part. Phys. Proc. 282-284 (2017) 149–152. doi:10.1016/j.nuclphysbps.2016.12.028.

[2] B. R. Webber, A QCD Model for Jet Fragmentation Including Soft Gluon Interference, Nucl. Phys. B238 (1984) 492–528. doi:10.1016/0550-3213(84)90333-X.

[3] B. Andersson, G. Gustafson, G. Ingelman, T. Sjostrand, Parton Fragmentation and String Dynamics, Phys. Rept. 97 (1983) 31–145. doi:10.1016/0370-1573(83)90080-7.

[4] Y. L. Dokshitzer, G. Marchesini, B. R. Webber, Nonperturbative effects in the energy energy correlation, JHEP 07 (1999) 012. arXiv:hep-ph/9905339, doi:10.1088/1126-6708/1999/07/012.

[5] Z. Tulipánt, A. Kardos, G. Somogyi, Energy–energy correlation in electron–positron annihilation at NNLL + NNLO accuracy, Eur. Phys. J. C77 (11) (2017) 749. arXiv:1708.04093, doi:10.1140/epjc/s10052-017-5320-9.

[6] G. Somogyi, Z. Trocsanyi, V. Del Duca, A Subtraction scheme for computing QCD jet cross sections at NNLO: Regularization of doubly-real emissions, JHEP 01 (2007) 070. arXiv:hep-ph/0609042, doi:10.1088/1126-6708/2007/01/070.

[7] G. Somogyi, Z. Trocsanyi, A Subtraction scheme for computing QCD jet cross sections at NNLO: Regularization of real-virtual emission, JHEP 01 (2007) 052. arXiv:hep-ph/0609043, doi:10.1088/1126-6708/2007/01/052.

[8] V. Del Duca, C. Duhr, A. Kardos, G. Somogyi, Z. Szőr, Z. Trócsányi, Z. Tulipánt, Jet production in the CoLoRFulNNLO method: event shapes in electron-positron collisions, Phys. Rev. D94 (7) (2016) 074019. arXiv:1606.03453, doi:10.1103/PhysRevD.94.074019.

[9] V. Del Duca, C. Duhr, A. Kardos, G. Somogyi, Z. Trócsányi, Three-Jet Production in Electron-Positron Collisions at Next-to-Next-to-Leading Order Accuracy, Phys. Rev. Lett. 117 (15) (2016) 152004. arXiv:1603.08927, doi:10.1103/PhysRevLett.117.152004.

[10] D. de Florian, M. Grazzini, The Back-to-back region in e+ e- energy-energy correlation, Nucl. Phys. B704 (2005) 387–403. arXiv:hep-ph/0407241, doi:10.1016/j.nuclphysb.2004.10.051.

[11] P. D. Acton, et al., A Determination of alpha-s (M (Z0)) at LEP using resummed QCD calculations, Z. Phys. C59 (1993) 1–20. doi:10.1007/BF01555834.

[12] A. Kardos, S. Kluth, G. Somogyi, Z. Tulipánt, A. Verbytskyi, Precise determination of $\alpha_S(M_Z)$ from a global fit of energy–energy correlation to NNLO+NNLL predictions, Eur. Phys. J. C78 (6) (2018) 498. arXiv:1804.09146, doi:10.1140/epjc/s10052-018-5963-1.

[13] T. Gleisberg, S. Hoeche, F. Krauss, M. Schonherr, S. Schumann, F. Siegert, J. Winter, Event generation with SHERPA 1.1, JHEP 02 (2009) 007. arXiv:0811.4622, doi:10.1088/1126-6708/2009/02/007.

[14] J. Bellm, et al., Herwig 7.0/Herwig++ 3.0 release note, Eur. Phys. J. C76 (4) (2016) 196. arXiv:1512.01178, doi:10.1140/epjc/s10052-016-4018-8.

[15] F. James, M. Roos, Minuit: A System for Function Minimization and Analysis of the Parameter Errors and Correlations, Comput. Phys. Commun. 10 (1975) 343–367. doi:10.1016/0010-4655(75)90039-9.

[16] J. M. Butterworth, A. R. Davison, M. Rubin, G. P. Salam, Jet substructure as a new Higgs search channel at the LHC, Phys. Rev. Lett. 100 (2008) 242001. arXiv:0802.2470, doi:10.1103/PhysRevLett.100.242001.

[17] D. Krohn, J. Thaler, L.-T. Wang, Jet Trimming, JHEP 02 (2010) 084. arXiv:0912.1342, doi:10.1007/JHEP02(2010)084.

[18] S. D. Ellis, C. K. Vermilion, J. R. Walsh, Recombination Algorithms and Jet Substructure: Pruning as a Tool for Heavy Particle Searches, Phys. Rev. D81 (2010) 094023. arXiv:0912.0033, doi:10.1103/PhysRevD.81.094023.

[19] S. D. Ellis, C. K. Vermilion, J. R. Walsh, Techniques for improved heavy particle searches with jet substructure, Phys. Rev. D80 (2009) 051501. arXiv:0903.5081, doi:10.1103/PhysRevD.80.051501.

[20] M. Dasgupta, A. Fregoso, S. Marzani, G. P. Salam, Towards an understanding of jet substructure, JHEP 09 (2013) 029. arXiv:1307.0007, doi:10.1007/JHEP09(2013)029.

[21] A. J. Larkoski, S. Marzani, G. Soyez, J. Thaler, Soft Drop, JHEP 05 (2014) 146. arXiv:1402.2657, doi:10.1007/JHEP05(2014)146.

[22] J. Baron, S. Marzani, V. Theeuwes, Soft-Drop Thrust, JHEP 08 (2018) 105. arXiv:1803.04719, doi:10.1007/JHEP08(2018)105.

[23] A. Kardos, G. Somogyi, Z. Trócsányi, Soft-drop event shapes in electron–positron annihilation at next-to-next-to-leading order accuracy, Phys. Lett. B786 (2018) 313–318. arXiv:1807.11472, doi:10.1016/j.physletb.2018.10.014.